BELLCOMM, INC.
955 L'ENFANT PLAZA NORTH, S.W. WASHINGTON, D.C. 20024

COVER SHEET FOR TECHNICAL MEMORANDUM

TITLE- An Evaluation of Various Strategies for Implementing a Minimum-Fuel, Attitude-Hold Control Mode for the AAP Orbital Workshop

TM-69-1022-10

DATE- September 30, 1969

FILING CASE NO(S)- 620

AUTHOR(S)- J. J. Fearnsides

FILING SUBJECT(S)- (ASSIGNED BY AUTHOR(S)-
Spacecraft Attitude Control
Optimal Control
Apollo Applications Program (AAP)

ABSTRACT

The existence of a minimum-fuel, steady-state attitude control mode for the AAP "Wet" Workshop was established in a previous paper. In this mode, the spacecraft is commanded to track a small, three-axis oscillation about the origin of an inertial reference frame rather than trying to align the spacecraft axes with the axes of the reference frame. In particular, the minimum fuel mode is a small, three-axis oscillation about the POP orientation in which the symmetry axis of the vehicle is aligned with an axis which is perpendicular to the orbital plane.

Subsequent to the publication of the aforementioned paper, several methods of implementing this mode with only minor changes to the existing design were suggested. This paper presents the details of an evaluation of these methods.

The first phase of the evaluation is concerned with the development of the analytical and geometrical properties of an optimal implementation of the minimum-fuel mode. These properties are then compared with the properties of the easily-implemented methods. Next, a comparison of these methods with the original design was performed using a full-scale digital simulation.

The principal result of the second phase of the study was that the use of any of these methods will result in a reduction in controller activity of 40 to 50 per cent of that achieved with the original design. For a reaction control

ABSTRACT (cont.)

system this reduction is achieved for both propellant consumption and the number of thrustor firings. Next, it is shown that if the techniques which were used to achieve this performance were applied to the first AAP "dry" workshop, further reductions in controller activity would result. Finally, the analytical and geometrical tools developed in the first phase of the report are used to show how further performance improvements could be made.

TABLE OF CONTENTS

BELLCOMM, INC.
955 L'ENFANT PLAZA NORTH, S.W. WASHINGTON, D. C. 20024

SUBJECT: An Evaluation of Various Strategies for Implementing a Minimum-Fuel, Attitude-Hold Control Mode for the AAP Orbital Workshop - Case 620

DATE: September 30, 1969

FROM: J. J. Fearnsides

TECHNICAL MEMORANDUM

1.0 INTRODUCTION

Steady-state reaction control of the attitude of a spacecraft in the presence of environmental disturbance torques is usually accomplished by using the thrustors to establish limit cycle motion of acceptable amplitudes about all three axes. For such strategies, the greatest lower bound for the propellant consumption is proportional to the integral over time of the absolute value of the total disturbance torque. A previous paper [1] showed that, when the disturbances are periodic, the environment itself is capable of producing an oscillatory motion about the spacecraft axes. These oscillations were considered to be "natural" limit cycles of spacecraft motion, that is, all turning points (zero-rate points) were produced by the disturbing torques. It was asserted that, if the control system could be used to track this motion instead of forcing its own limit cycle motion, the greatest lower bound of propellant consumption would be reduced. In particular, the attitude hold mode of the Orbital Workshop (OWS) of the Apollo Applications Program (AAP) was shown to be subject to periodic gravity-gradient and aerodynamic disturbance torques during missions AAP 1/2 and AAP 2/3A. The corresponding equations of motion were shown to possess a periodic solution and the amplitudes of these oscillations ("natural" limit cycles) to be approximately 10 deg., 4 deg. and 4 deg. respectively for the roll, pitch, and yaw axes. The greatest lower bound of propellant consumption for steady-state attitude control was shown to be zero.

Subsequent work [2] demonstrated the uniqueness of the solutions obtained in [1] and presented an algorithm for the determination of the initial point on the state-space trajectory of these solutions. This algorithm can be used to generate a point-by-point "desired trajectory" in the state space and defines a moving target point for the control problem stated below.

Control Problem

Given the dynamical system represented by the equation

$$\dot{\underline{x}} = F(t)\underline{x} + \underline{z}(t) + G(t)\underline{u} \ , \qquad (1)$$

the target point $\underline{x}_p(t)$ defined by the previously cited algorithm and the characteristics of the controller (an on-off, reaction thrust system), determine the control which takes an arbitrary point in state space to the desired trajectory (target point) with a minimum expenditure of propellant.

The purpose of this paper is to present the results obtained in an investigation of this control problem for the roll axis (in this case, the axis of minimum moment of inertia) of the OWS. There is ample justification for restricting the the problem in this way:

(1) In the limit cycle control strategy originally considered for the OWS [3], the propellant requirement for roll-axis control was 70% of the total requirement for all three axes.

(2) The linearized equation of roll motion is uncoupled from the pitch and yaw equations.

(3) The roll axis is unaffected (to first order) by the aerodynamic torque. This represents a considerable simplification in the definition of the target set.

Section 2 contains the equation which describes the roll axis motion, the definitions of the steady-state control problem, the regulation problem and the acquisition problem, and some thoughts on the optimal solution of the regulation problem. Section 3 includes the description and evaluation of two sub-optimal control laws. Their properties are compared with the properties of the "optimal" solution and their performance is compared with the performance of the original design of the Workshop Attitude Control System (WACS). Section 4 is a summary and Section 5 considers the difference in performance between the so-called "wet" and "dry" workshops.

Appendix A is a discussion of the linearization techniques used to develop the equations for the regulation problem. Appendix B lists some pertinent properties of the solutions of Mathieu equations. Appendix C includes a statement of the Minimum Principle of Pontryagin.

2.0 ROLL AXIS OPTIMAL CONTROL

2.1 Equations of Motion

The linearized equation describing roll-axis motion in the absence of a control torque was given in [1] as

$$\ddot{\psi} = 2\alpha_z^2 \psi \cos 2\omega_o t - \alpha_z^2 \sin 2\omega_o t , \qquad (2)$$

where ψ = the Euler angle rotation about the axis of minimum moment of inertia of the spacecraft

$$\ddot{\psi} = \frac{d^2\psi}{dt^2}$$

ω_o = the orbital rate, rad/sec

$$\alpha_z^2 = 1.5\ \omega_o^2\ \frac{|I_x - I_y|}{I_z}$$

I_j, j = (x,y,z) = the moments of inertia about the principal axes of the spacecraft.

The equations (1) have since been updated to include the effects of a nondiagonal inertia tensor and all nonlinear terms which were greater than 2% of the maximum value of $\ddot{\psi}$ as given by the solution of equation (2). Fortunately, this new equation for ψ is uncoupled and is

$$\ddot{\psi} = 2\gamma_z^2 \psi [\cos 2(\omega_o t - \delta)] - \gamma_z^2 \sin 2(\omega_o t - \delta) - \lambda_B \qquad (3)$$

where γ_z^2 is slightly greater than α_z^2 since it includes the additional gravity gradient torque when the geometric axes are controlled, $\delta \simeq 8$ deg. is a measure of the angular separation of the principal and geometric axes, and λ_B is a constant which is coupled into the roll equation from the pitch axis and due to the "diurnal bulge" in the atmospheric density.

Consider now, the linear dynamical system [4,5] given by

$$\dot{\underline{x}} = F(t)\underline{x} + \underline{z}(t) + \underline{u}(t) \qquad (4)$$

where $\underline{x}$ is a 2 x 1 state vector,

$F(t)$ is a 2 x 2 matrix,

$\underline{z}(t)$ and $\underline{u}(t)$ are respectively 2 x 1 vectors of environmental and control forcing terms.

System (4) is equivalent to (3) if,

$$\underline{x} = \begin{bmatrix} x_1 \\ x_2 \end{bmatrix} = \begin{bmatrix} \psi \\ \dot{\psi} \end{bmatrix},$$

$$F(t) = \begin{bmatrix} 0 & 1 \\ 2\gamma_z^2 \cos 2(\omega_o t - \delta) & 0 \end{bmatrix},$$

and

$$\underline{z}(t) = \begin{bmatrix} 0 \\ -\gamma_z^2 \sin 2(\omega_o t - \delta) - \lambda_B \end{bmatrix}$$

2.2 The Steady-State Control Problem

The steady-state control problem is defined as follows: Given perfect sensors and complete knowledge of the system

dynamics and of the characteristics of the environment, determine the control law

$$\underline{u}_{ss}(t) = \underline{k}_{ss}(\underline{x}(t),t) \tag{5}$$

which keeps the motion (x_1,x_2) of system (4) within acceptable bounds and which minimizes the propellant consumption.

This is obviously an ad-hoc definition. In particular, no precise target set is defined. This is done in order to utilize the results of [1]. That is, since $F(t)$ and $\underline{z}(t)$ are still periodic, the algorithm presented in [2] applies. It produces the initial vector which yields a periodic solution, $\underline{x}_p$, to the initial value problem

$$\dot{\underline{x}} = F(t)\underline{x} + \underline{z}(t), \quad \underline{x}(t_o) = \underline{x}_o \quad . \tag{6}$$

If the amplitude of this oscillation is acceptable, $\underline{x}_p$ is also a solution to the steady-state control problem. Further, the hypotheses of the definition of this problem imply that once this motion is achieved, no further control action is necessary to sustain it. That is, $\underline{u}_{ss}(t) = \underline{0}$.

2.3 The Regulation and the Acquisition Problems

Of course, these hypotheses, while very useful for determining the properties of the equivalent dynamical system, do not provide an adequate description of the physical situation. There are sensor errors and the mathematical models of plant dynamics and controller characteristics are incomplete. Also, the properties of the environment, even if perfectly known, are always changing. Thus, the actual state of the system, $\underline{x}(t)$, will not always coincide with the desired state, $\underline{x}_p(t)$, and some control action will be necessary to keep the quantity, $\underline{\varepsilon} = \underline{x} - \underline{x}_p$, small. Notice that the desired trajectory will define a moving target point for the control problem which was presented in Section I and which is repeated in a more general form below.

Control Problem - Given the dynamical system represented by

$$\dot{\underline{x}} = \underline{f}(\underline{x}(t), \underline{z}(t), \underline{u}(t), t) \tag{7}$$

and the target set

$$\tilde{S} = \left\{ \underline{x} : \underline{x} = \underline{x}_d(t) \right\}$$

where $\underline{x}_d(t)$ is the periodic solution of (7) with $\underline{u}(t) = \underline{0}$, determine the control law

$$\tilde{\underline{u}} = \tilde{\underline{k}} \, [\underline{x}(t), t] \tag{8}$$

which takes the phase[1] of the system from an arbitrary point $(\underline{x}_o, t_o)$ into $\tilde{S}$ with a minimum expenditure of propellant.

This problem is stated in general terms to motivate the following definitions of the acquisition problem and the regulation problem. The key word in the statement is arbitrary. If (8) must take an arbitrary phase point to the target set then (7) must be used to describe system dynamics rather than the linearized version (1). That is, a proper model of the roll axis motion would be nonlinear. It also would be coupled to the equations describing pitch and yaw motions. This requires analysis in a six-dimensional state space rather than the two-dimensional space which can be used when the equations are uncoupled.

The above, coupled with the fact that the solution of this general control problem requires a controller which corrects large and small errors in an efficient manner, leads to a further sub-division of the control problem. These subdivisions are called the acquisition problem and the regulation problem and are defined below.

---

[1] A phase space is a state space which has been augmented by the addition of the time axis. A phase point is an element of the phase space. The expression "the phase of the system $(\underline{x}_o, t_o)$" is preferable to "the state of the system $\underline{x}_o$ at time t_o". More precisely, if the state of the system is described by points in an n-dimensional Euclidean space R^n and if R is the set of all real numbers, elements of the phase space are points in the space defined by the Cartesian product $R^n \times R$.

THE ACQUISITION PROBLEM [6]

Given: the dynamical system

$$\dot{\underline{y}} = \underline{g}(\underline{y}(t), \underline{\zeta}(t), \underline{\nu}(t), t)$$

where $\underline{y}(t)$ is the 6 x 1 vector describing the state of the entire three-axis system, and $\underline{\zeta}(t)$ and $\underline{\nu}(t)$ are vector models of the environmental and the control influences, respectively; and the fixed target set $\xi \supset \tilde{S}$, find the control

$$\underline{\nu}(t) = (\underline{y}(t), t)$$

which takes this system from an arbitary phase point $[\underline{y}_o, t_o]$ into the phase space $[\xi, t_1]$ for some $t_1 > t_o$.

Obviously, the function of the acquisition control mode is to make large attitude and rate corrections and bring the state of the system into the proximity of the desired state. The target set ξ should be small enough in all six-dimensions of the state space to assure that the roll axis equation can still be considered uncoupled yet large enough to include $\tilde{S}$. Finally, a minimum-fuel performance criterion is unnecessary since the regulation control mode will keep the trajectory inside ξ.

THE REGULATION PROBLEM

Given the dynamical system described by

$$\dot{\underline{x}} = \underline{f}(\underline{x}(t), \underline{z}(t), \underline{u}(t), t) \qquad (7)$$

and the target set $\tilde{S} = \{\underline{x} : \underline{x} = \underline{x}_d(t) \subset \xi\}$ determine the admissible control law

$$\hat{\underline{u}}(t) = k(\underline{x}(t), t) \ , \qquad (8)$$

which takes the state of the system from a phase point $[\underline{x}_o, t_o] \in [\xi \text{ X } T]$ into the phase point $[x_d(t_1), t_1] \in [\tilde{S} \text{ X } T]$ and minimizes the performance functional

$$J(\underline{u}) = \int_{t_o}^{t_1} L(\underline{x},\underline{u},t)dt = \int_{t_o}^{t_1} |\underline{u}|dt, \quad t_1 \text{ unspecified.} \qquad (9)$$

Note that the minimum propellant criterion is given more precise definition. The concept of an admissible control law [7] for this problem merely implies that the given controller must be able to perform the required functions. Finally, and most importantly, the set ξ should be chosen such that the equivalent dynamical system equation for the regulation problem can be approximated by

$$\dot{\underline{\varepsilon}} = F(t)\underline{\varepsilon} + G(t)\underline{u}(t) \quad , \qquad (10)$$

where $\underline{\varepsilon}$ measures the deviation of the actual system state from the desired state. The details of this linearization are presented in Appendix A.

2.4 A Minimum Fuel Regulator

The linearized equation for small variations of roll axis motion about the desired trajectory is shown in Appendix A to be

$$\ddot{w} - (2\alpha_z^2 \cos 2\omega_o t)w = Nu(t) \qquad (11)$$

where N = the magnitude of the control torque divided by I_z and the maximum value of $|u(t)| = 1$. It will be convenient to adjust the time scale by the substitution $\tau = \omega_o t$ which yields

$$\frac{d^2w}{d\tau^2} = w'' = (2q \cos 2\tau)w + \lambda u(\tau) \quad . \qquad (12)$$

The homogeneous equation corresponding to (12) is

$$w''-(2q\cos 2\tau)w = 0 \qquad (13)$$

and is a Mathieu equation. The properties of solutions to (13) are well known [8] and most interesting. In addition, they will be very helpful in the determination of the optimal control for the regulation problem. The pertinent properties of Mathieu equations are presented in Appendix B. Of primary importance is the fact that, for values of q in the vicinity of the q which corresponds to our particular problem, solutions to (13) are uniformly stable [9]. This is demonstrated with the help of Figure 1 which presents the state-space trajectories of two independent solutions $w_1(t)$ and $w_2(t)$ of (13) when q is taken to be 0.68. $w_1(t)$ is the response to the initial conditions $w_1(0) = 1$, $w_1'(0) = 0$; and $w_2(t)$ the response to the initial conditions $w_2(0) = 0$, $w_2'(0) = 1$. Any solution, $v(t)$, of (13) can be expressed as a linear combination of $w_1(t)$ and $w_2(t)$ and is bounded for any finite initial state and any initial time. In addition, the form of the trajectories in Figure 1 suggests that a fuel-optimal control for this system might be similar to the optimal control of the linear harmonic oscillator. This view is reinforced by the following example.

EXAMPLE 1.

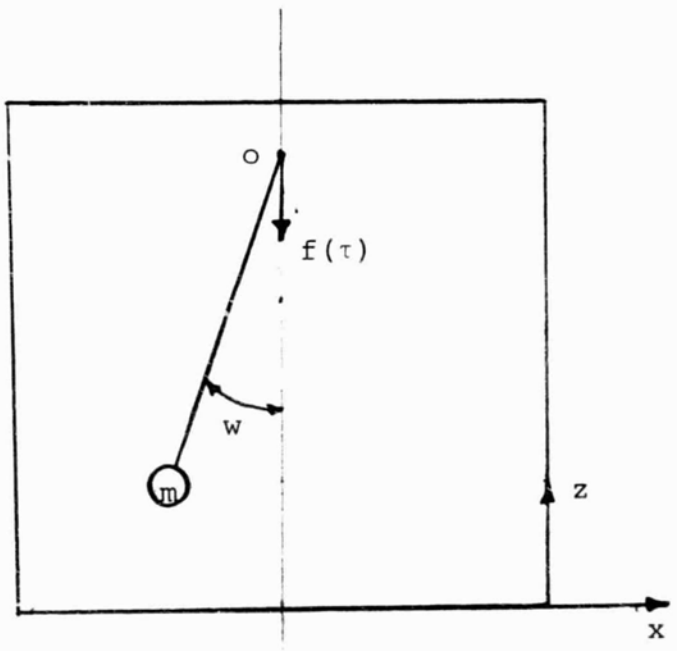

Sketch 1.

Consider that both the mass, m, and the support, o, of the pendulum shown in sketch 1 are in the horizontal plane xz. That is, xz represents a table-top which will be considered frictionless with respect to the motion of m. In addition, the support will be free to move along the z axis. The rod of the pendulum is, of course, light and inextensible. The question now posed is: what is the equation describing small, rotational motions of m in response to forces $f(\tau)$ in the z direction and applied at the support? It is easily seen that

$$w'' = \frac{f(\tau)L}{I} \sin w \approx \frac{f(\tau)}{I} Lw$$

where L = the moment arm and

I = the moment of inertia of m about o.

Choosing $\frac{L}{I} f(\tau) = \left(2q\cos(2\tau) \right)$ yields (13). Notice that there is no applied torque when $w = 0$.

The intuitive nature of the preceding was presented to provide physical insight to the solution of the problem which will now be attacked more formally. Appendix C contains a statement of the necessary conditions for fuel-optimal control of (10) as given by the Minimum Principle of Pontryagin [5]. The resulting control law,

$$u^*(t) = \begin{cases} 0, & |p_2^*| < 1 \\ -1, & p_2^* > 1 \\ 1, & p_2^* < -1 \end{cases}, \qquad (14)$$

gives the control as a function of the adjoint variable p_2^*. A relationship between the adjoint vector $\underline{p}^*$ and the state vector $\underline{x}^*$ is needed to complete the problem. This will be accomplished by a graphical analysis which is very similar to the approach taken to develop the time-optimal [5,7] and fuel-optimal [10,11] controls for a linear, unforced harmonic oscillator.

It is easy to show (C-7) that the terminal value of p_2^* must satisfy

$$p_2^*(t_1) = \begin{cases} -1, & \text{if } u^*(t_1) = +1 \\ +1, & \text{if } u^*(t_1) = -1 \end{cases} \tag{15}$$

and that $|u^*(t_1)| = 1$. The latter condition is due to the fact that no trajectory will "coast" into the origin and is easily seen in the characteristics of the solutions of the unforced Mathieu equations shown in Figure 1. This implies that the terminal segment of the optimal trajectory is the trajectory which corresponds to the solution of the forced Mathieu equation (12) with $u(t) = \pm 1$ and which intersects the origin of the state space. In the case of the linear harmonic oscillator whose motion is described by $\ddot{x} + x = 1$ the steady-state response to a constant forcing function defines a new equilibrium point at $x = +1$ about which the homogeneous solution oscillates. The terminal segment of the optimal trajectory is then determined graphically and is a segment of the optimal switching curve. The control is now given as a function of the state and the problem is complete. Unfortunately the Mathieu equation possesses no corresponding constant particular solution to (12). This fact makes the determination of the optimal switching lines more difficult from an analytical standpoint.

There is, however, a considerable amount of information on the fuel-optimal control of pendula with on-off controllers. In particular, Busch and Flügge-Lotz [11] showed that, for a system described by the standard form of the Mathieu equation (B-1), that control should be applied when the trajectory is in the vicinity of the vertical axis of the state space. A similar result was obtained by Flügge-Lotz and Craig [10] for the linear harmonic oscillator. The switching lines for the latter case are shown in Figure 2. The slope of these lines depends on the control torque λ, the initial conditions and the number of switchings which will be used to drive the trajectory to the origin of the state space. For the large control torques available in the WACS, these lines are essentially vertical for any initial condition which preserves the linearity of the mathematical model (12). This is easily demonstrated. Consider the state vector formulation of (12)

$$\dot{\underline{\varepsilon}} = F(\tau)\underline{\varepsilon} + G(\tau)u(\tau) \tag{16}$$

where the transpose of $\underline{\varepsilon}$ is given by

$$\underline{\varepsilon}^T = [w, w'] \quad ,$$

$$F(\tau) = \begin{bmatrix} 0 & 1 \\ 2q \cos 2\tau & 0 \end{bmatrix} \quad ,$$

$$[G(\tau)\underline{u}(\tau)]^T = [0, \lambda u(\tau)] \quad , \text{ and}$$

$$u(\tau) = \begin{cases} 1, & t_c < \tau < t_c + \Delta\tau \\ 0, & \text{elsewhere} \end{cases}$$

where $\tau = t_c$ defines the instant of control application.

The representation formula [2] for a solution $\phi(\tau)$ of (16) is given by

$$\underline{\phi}(\tau) = \Phi(\tau, 0)\underline{\phi}(0) + \int_0^\tau \Phi(0, \sigma)\, G(\sigma)\underline{u}(\sigma)\, d\sigma$$

In particular the change of $\underline{\phi}(\tau)$ during the short firing interval $\Delta\tau$ is desired. Since the transition function of a dynamical system is continuous, the value of $\underline{\phi}(t_c-)$, where t_c- defines the instant before the control is applied, is given by

$$\underline{\phi}(t_c-) = \Phi(t_c, 0)\underline{\phi}(0) \quad .$$

The change in $\underline{\phi}(\tau)$ upon application of $G(\tau)\underline{u}(\tau) = \underline{\lambda}(\tau)$ is

$$\underline{\phi}(t_c+\Delta\tau) = \Phi(t_c+\Delta\tau, t_c)\underline{\phi}(t_c-) + \int_{t_c}^{t_c+\Delta\tau} \Phi(t_c,\sigma)\underline{\lambda}(\sigma)d\sigma \quad .$$

For $\Delta\tau$ very small, $\Phi(t_c+\Delta\tau, t_c) \simeq I$, the unit matrix, and

$$\int_{t_c}^{t_c+\Delta\tau} \Phi(t_c,\sigma)\underline{\lambda}(\sigma)d\sigma \simeq \Phi(t_c,t_c+\Delta\tau)\int_{t_c}^{t_c+\Delta\tau} \underline{\lambda}(\sigma)d\sigma$$

$$\simeq \int_{t_c}^{t_c+\Delta\tau} \underline{\lambda}(\sigma)d\sigma = \underline{\lambda}\Delta\tau \quad .$$

This implies that

$$\underline{\phi}(t_c+\Delta\tau) \simeq \underline{\phi}(t_c-) + \underline{\lambda}\Delta\tau \quad .$$

or

$$\begin{aligned} \phi_1(t_c+\Delta\tau) &= \phi_1(t_c-) \\ \phi_2(t_c+\Delta\tau) &= \dot{\phi}_1(t_c+\Delta\tau) = \phi_2(t_c-) + \lambda\Delta\tau \quad . \end{aligned} \tag{17}$$

Thus, for large values of the control torque, the optimal trajectories are defined as points on the line in the state space of system (12) defined by $w = 0$.

This result is shown to be physically satisfying by a consideration of Example 1. An impulsive torque applied when $w \neq 0$ does not remove the instantaneous potential energy.[1] The pendulum will, therefore, still experience a rotational motion.

---

[1] That is, $f(\tau)$ can be considered to be the negative gradient of some generalized potential energy function.

If the state of system (1) is once again referred to the origin of the state space $\underline{x} = 0$ instead of to the desired trajectory, the control law is as shown in Figure 3. This result will be used to evaluate the various sub-optimal schemes which are presented in the next section.

3.0 SUB-OPTIMAL STRATEGIES

The implementation of a control strategy based on the ideas presented in [1] is quite involved. It has just been shown that even the relatively uncomplicated roll axis motion would require a digital control computer for proper implementation of the optimal strategy. However, two sub-optimal schemes have been proposed which are both simple enough to be mechanized by an analog computer and effective relative to the performance of the original WACS control law. The first of these, suggested by H. E. Worley[1], just involves opening the deadband of a simple position-plus-rate feedback control law such that the optimal trajectory is a subset of the region interior to the switching lines. This will be discussed in Section 3.1. An alternate approach, first suggested by J. Kranton of Bellcomm and then, independently, by D. N. Schultz[2] involves the generation of a sinusoidal command attitude as an approximation to the desired trajectory, $\underline{x}_p(t)$, of (3). A position-plus-rate feedback control law keeps the actual trajectory close to the commanded trajectory. This approach, called the sinusoidal trajectory method, is considered in Section 3.2. Section 3.3 will be concerned with an evaluation and comparison of the two methods.

3.1 The Expanded Deadband Method (EDM)

The position-plus-rate feedback control law mentioned above is illustrated in Figure 4. It has received wide acceptance by designers of on-off spacecraft attitude control systems for many years (see, for example, [12]), because of its stability properties. The switching lines, Γ_1 and Γ_2, separate the state space of the system into a powered region and a coasting (or deadband) region. The powered region is further sub-divided into positive and negative torque regions. x_o and $\dot{x}_o$ define the attitude and rate crossover points, respectively. The control logic defined by these switching lines is as follows:

---

[1] S&E-AERO-DDD, Marshall Space Flight Center, Huntsville, Alabama.

[2] S&E-ASTR-NGA, Marshall Space Flight Center, Huntsville, Alabama.

1. Define $e_n = a_o x + a_1 \dot{x}$ where e_n is a composite error signal formed by a linear combination of the instantaneous attitude and rate signals.
2. Let $a_o = 1/x_o$ and $a_1 = 1/\dot{x}_o$
3. The inequality $|e_n| < 1$ defines the deadband (coasting region), $e_n > 1$, defines the negative torque region and $e_n < -1$ defines the positive torquing region. The equalities $e_n = \pm 1$ define the switching lines Γ_1 and Γ_2.

If $a_o = 2$ and $a_1 = 20$, the above constitutes an adequate description of the control law originally designed for the WACS [3]. This will be called the nominal strategy [13]. Notice that $a_o = 2$ implies that the thrustors will fire when $|x| > 0.5$.[1] The limit cycle motion which results from the nominal strategy is much smaller than the "natural" limit cycle described in [1]. It has a smaller average attitude error but is relatively expensive of propellant since it takes no advantage of the "free-ride" that the environment can provide.

The expanded deadband method, shown in Figure 5, results from setting $a_o = .067$ and $a_1 = 28.6$. The desired trajectory, represented by S, is now fully within the coasting region, Γ. Put more formally, if

$$\Gamma = \left\{ x(t), \dot{x}(t) : |e_n(t)| = |a_o \dot{x}(t) + a_1 x(t)| < 1 \right\}$$

and if

$$S = \left\{ x(t), \dot{x}(t), t : \underline{x}(t) = \begin{bmatrix} x(t) \\ \dot{x}(t) \end{bmatrix} = \underline{x}_p(t) \right\} ,$$

then $S \subset \Gamma$. Note that this strategy only constrains the state of the system to stay within Γ, a fixed target set. There is no such convergence to the moving target point $\underline{x}_p(t)$ as could

---

[1] The rate signal has almost no effect in this case.

be provided by the optimal strategy illustrated in Figure 3. However, the switching lines in the expanded deadband method make much better use of the "free-ride" capabilities than the nominal method by providing tight control only in the first and third quadrants where the state would accelerate out of Γ. The expanded deadband method was evaluated with full-scale simulation [13] of the equations of motion of the OWS. The resulting roll-motion over five orbits of this simulation is presented in Figure 6. It is seen that this control law keeps the state of the system near the fixed target set, S, but provides no convergence to the moving target point, $\underline{x}_p(t)$. A discussion of the propellant consumption associated with the expanded deadband method is given in Section 3.3.

3.2 The Sinusoidal Trajectory Method (STM)

The generation of the true desired trajectory, while of great interest as an abstraction, is really unnecessary for application to the OWS because of the practical limitations of the system. For example, the thrust levels of the WACS can deviate as much as 4% from the specified nominal thrust. This suggests the possibility of developing a moving target point by generating a sinusoidal command angle and rate. Since the phase of the sinusoids can be adjusted to compensate for orbital regression, the concepts expressed in [1] could be integrated into an analog system. Further, if the nominal control strategy (Figure 4) were used with the error being measured relative to the sinusoidal trajectory, this method could be integrated into the WACS.

Figures 7 and 8 illustrate two possible implementations of this method which will be called STMI and STMII. The rate axis is scaled to allow the sinusoidal trajectory $\underline{x}_s(t)$ to be circular. The slopes of the switching lines are adjusted appropriately and give a better indication of the almost insignificant amount of rate feedback in the nominal control law. Figure 8 differs from Figure 7 in that only the attitude is commanded; the rate command is zero.

In summary,

1) define $\underline{x}_{s1}(t) = \begin{bmatrix} \psi_{max}\sin 2(\omega_o t + \sigma^*) \\ 2\omega_o \psi_{max}\cos(\omega_o t + \sigma^*) \end{bmatrix} = \begin{bmatrix} x_{s_1}(t) \\ \dot{x}_{s_1}(t) \end{bmatrix}$

$$\underline{x}_{s2}(t) = \begin{bmatrix} \psi_{max}\sin 2(\omega_o t + \sigma^*) \\ 0 \end{bmatrix} = \begin{bmatrix} x_{s_2}(t) \\ \dot{x}_{s_2}(t) \end{bmatrix}$$

2) define the error signals $e_{s1}(t)$ and $e_{s2}(t)$ as follows:

$$e_{s1}(t) = a_o\left(x(t)-x_{s1}(t)\right) + a_1\left(\dot{x}(t)-\dot{x}_{s1}(t)\right)$$

$$e_{s2}(t) = a_o\left(x(t)-x_{s2}(t)\right) + a_1\dot{x}(t)$$

3) Figure 7 represents the nominal control law described in Section 3.1 if $e_n(t)$ is replaced by $e_{s1}(t)$.
Figure 8 represents the control law which results from the substitution of $e_{s2}(t)$ for $e_n(t)$.

The moving target point is shown at three instants of time in each figure. Note that the switching lines move in synchronism with the desired trajectory in the $\underline{x}$ plane. If the error equations are written as

$$e_{s1}(t) = a_o w_{s1}(t) + a_1 \dot{w}_{s1}(t) \quad ,$$

$$e_{s2}(t) = a_o w_{s2}(t) + a_1 \dot{w}_{s2}(t)$$

then, with respect to the $\underline{w}_{s1}$ and $\underline{w}_{s2}$ planes, the control law representation takes the form of Figure 4 and, as discussed in Section 2, is a control strategy for the regulation problem. Several important observations can be obtained by close scrutiny of these Figures.

First, it is noticed that, due to the paucity of rate-feedback, there is no essential difference in the two approaches. This is illustrated in Figure 7 by extending the switching lines around $\underline{x}_{s1}(t_o+n\pi/\omega_o)$ to intersect the $\dot{x} = 0$ axis. This extension is shown dotted. The solid lines adjacent and parallel to the dotted lines represent the switching lines about $x_{s2}(t_o+n\pi/\omega_o)$. Therefore, if the constants a_o and a_1 are constrained, the second method is preferable since it requires only one generator. Further comparisons between these two methods are presented in Section 3.3.

It was mentioned in Section 2 that the general control problem was subdivided because the thrustor impulses required for acquisition would likely be too large for efficient regulation. This is now shown with the help of Figure 8. For the WACS to perform a pure roll motion two thrustors must be fired. Firing a single thrustor produces a combined roll and yaw motion. The change in OWS roll rate ($\Delta\dot{x}_2$) achieved by the minimum impulse bit of two WACS thrustors (MIB_2) is approximately .0065 deg./sec. This is graphically represented in the upper left of Figure 8 and is seen to be rather large for fine control. Fortunately, for the OWS, the moment of inertia about the yaw axis is considerably larger (about 13:1) than the moment of inertia about the roll axis. Finer control can then be achieved with minimal adverse effects if only one thrustor is fired. The $\Delta\dot{x}_1$ corresponding to (MIB_1) is shown in the upper right hand side of Figure 8.

The preceding paragraph was interjected to assist in explaining what might be expected if a_o and a_1 were changed in such a way as to increase the effect of the rate feedback. Two points become immediately apparent. First, the two methods described above are no longer similar. Secondly, the attitude accuracy must be decreased because a_o must be reduced. This is because, if the rate feedback were increased by keeping a_o constant and increasing a_1, an application of the minimum impulse bit MIB_1 would cause the state trajectory to contact the opposite side of the deadband. For this reason, a_o was chosen to be 0.7 and a_1 to be 200. The results of two simulation runs using these values are presented in the next section.

Finally, it is noted that the fuel savings achieved by both the expanded deadband method (EDM) and the sinusoidal trajectory method (STM) are due to their success in holding the spacecraft close to the solution of the steady-state control problem. That is, the EDM has no provision for solving the regulation problem and the STM provides a non-optimal solution. These observations demonstrate the usefulness of separating the control problems as was done in Section 2 rather than trying[1] to apply optimization techniques directly to the forced system.

3.3 Simulation Results

Several variations of the two sub-optimal methods (EDM, STM) were tested on a three-axis digital simulation of

---

[1] No generalization is implied here to systems with different types of forcing functions.

the dynamics of the OWS in the presence of gravity-gradient and aerodynamic disturbance torques and controlled by the WACS. While there are tradeoffs among possible sub-optimal designs, the principal result was that all of the candidate methods were more economical of propellant consumption and number of thrustor firings than was the nominal method (Figure 4.).

Table 1 presents the important results obtained with the previously cited digital simulation in which several cases of the nominal method (Nom.), the EDM and the STM were run for 20 orbits. The significance of the column headings is as follows:

i. Define a general error signal,

$$e(t) = a_o(x-x_c) + a_1(\dot{x}-\dot{x}_c) \qquad (18)$$

where $x_c = x_c(t)$ and $\dot{x}_c = \dot{x}_c(t)$ define the desired trajectory.

ii. a_o and a_1 are obvious from (18).

iii. COM = 0 means that the error is measured from the geometric axes of the spacecraft ($x_c, \dot{x}_c = 0$). COM = 1 means that the error is measured from the spacecraft principal axes (x_c = constant, $\dot{x}_c = 0$). COM = 2 is used for method STMI and COM = 3 for STMII. COM = 4 represents a variation of method STMI where $x_c = A\sin 2(\omega_o t - 7.77°)$. A is taken to be 10 for all cases.

iv. CNTRL = 1 combines the roll and yaw error signals so that one thrustor may be fired for roll control. CNTRL = 2 signifies that each axis is controlled individually and, therefore, two thrustors are fired for roll control.

v. TOTAL NO. OF FIRINGS gives the total number of thrustor engine firings in 20 orbits. For example, STM case 1, shows 722 in this column. There are six thrustors in the WACS

TABLE I

Controller Activity For Several Control Laws

Control Law	Case	a_o	a_1	COM	CNTRL	Total No. Of Firings	Avg. No. Fir. Per Orbit	Prop. Cons. Per Orbit in pounds (#)	84-Day Totals	
									Prop. Cons. (#)	No. Firings
Nom.	1	2	20	1	1	1375	68.75	.344	462	92,400
Nom.	2	2	20	0	1	1425	71.25	.356	479	95,760
EDM	1	0.067	28.6	1	1	735	36.75	.184	247	49,392
EDM	2	0.067	28.6	0	1	823	41.15	.206	277	55,306
EDM	3	0.067	28.6	1	2	745	37.25	.186	250	50,064
STMI	1	2	20	2	1	722	36.10	.181	243	48,518
STMII	2	2	20	3	1	764	38.20	.191	258	51,341
STMI	3	0.7	200	2	1	764	38.20	.191	251	51,341
STMI	4	0.7	200	4	1	680	34.00	.170	228	45,696

and, for this case, the distribution of this total over the individual thrustors is 66, 122, 158, 156, 73 and 147.

vi. The next column, AVG. NO. FIR. PER ORB., just divides the previous column by 20.

vii. Column heading PROP. CONS. PER ORB. gives the average propellant consumed per orbit in pounds (#). In the attitude-hold mode all firings were minimum impulse bits of 1.25 # sec. For this reason the MIB value of 250 sec was used for the specific impulse.

viii. Finally, the last two columns give the total propellant consumption and number of thrustor firings over the combined duration of the AAP 1/2 and AAP 2/3A missions. The number of orbits per day was considered to be 16.

A comparison of the first four cases indicates that less propellant is consumed when the principal axes of the spacecraft are controlled rather than the geometric axes. This is due to the additional gravity-gradient torque acting on the vehicle when the principal axes are not aligned. However, principal axis control has the disadvantage that the solar panels are not optimally oriented when the error is zero. Thus, for the nominal case, the solar panels are kept at 7.77 deg + 0.5 deg. from the optimal position and for EDM case 1, the $\bar{v}$ector normal to the plane of the panels oscillates between 22.77 deg. and -7.23 deg. rather than between $\pm$15 deg. EDM case 3 was inserted to show the performance degradation when the roll control is independent of yaw control. This degradation is more pronounced when the deadband is smaller.

One of the strong features of the STM is that the indicated performance was achieved while controlling the geometric axes. In addition, a comparison of STM cases 1 and 2 shows that, as predicted, the absence of a commanded rate does not seriously affect the performance. The tradeoff here is between performance and an extra generator.

STM cases 3 and 4 represent the results of a single effort to evaluate the performance characteristics with a greater amount of rate feedback. The values for _ and a_1 were chosen such that, in the worst case, a minimum impulse bit firing would not cause the state to contact the opposite side of the deadband. In particular, STM case 4 illustrates

the improvement in performance which results when the phase of the commanded signal is shifted by 7.77°, the angle corresponding to the roll axis angle separating the principal and geometric axes of the spacecraft. This effect, explained with the help of equation (3), represents an important property of the STM. That is, the phase of the desired trajectory can be adjusted to reduce the effect of the additional gravity-gradient torque which acts on the vehicle when the geometric axes are controlled. Thus, although the solar panels will not be optimally positioned at orbital noon, the vector normal to the panels will continue to experience an angular deviation relative to the optimal of approximately ± 10 deg. rather than, say, +3 deg. to -17 deg. An additional benefit of STM case 4 is that the firings are distributed more evenly over each of the individual thrustors. For example EDM case 1 has a distribution of firings over the six engines of {94, 104, 90, 149, 192, 106} while the corresponding distribution for STM4 is {76, 142, 134, 134, 94, 100}. Over 84 days this means that the most active thrustor will fire 3,360 fewer times. Finally, it should be reiterated that STM case 4 does not represent the "best" result of a full sensitivity analysis of a_o, a_1 and the amplitude and phase of the desired trajectory. It is merely a first effort based on the geometry of the switching curves.

4.0 SUMMARY

This paper is an extension of [1]. Together, they present the results of a study which was undertaken to determine ways of reducing WACS propellant consumption and the number of thrustor ignitions. A comparison of cases STM4 and Nom. 1 in Table 1 provides an indication of the success of the overall study; that is, a 50% reduction in controller activity.

It should be pointed out, however, that the theoretical and computational machinery presented in this paper were developed to provide even further improvements in system performance. For example, a simulation of the optimal control strategy, even if it were too complex for practical implementation, would have performed the function of establishing a criterion against which all sub-optimal strategies could be compared. Also, as previously mentioned, a sensitivity analysis of propellant consumption versus a_o and a_1 in the STM method in conjunction with the graphical concepts expressed in Section 3.2 may have resulted in further improvement in system performance. A desired trajectory formed by adding a constant to the sinusoidal trajectory may have been tried. Finally, desired trajectories or expanded deadbands for the pitch and yaw axis could have been developed to reduce controller activity even further.

The fact that the adoption of a "dry" workshop for AAP has also dictated control by control moment gyros rather than a reaction-thrust system does not automatically imply that the results presented here are useless. The definition of the steady-state control problem and the determination of the existence of its solution are of interest with any controller. This is expecially true for long duration missions since it provides a way of outsmarting the environment rather than overpowering it. Another important observation that emerges from this study is that knowledge of plant dynamics, the environments and controller characteristics must be considered in any meaningful control system design. Optimization by sensitivity analysis alone has many pitfalls.

5.0 EPILOGUE: THE DRY WORKSHOP

It is interesting to consider the performance characteristics of the solar astronomy dry workshop if it were controlled by the WACS and used the method described above. A preliminary estimate of the principal moments of inertia [14] is

$$I_x = 3{,}543{,}940 \text{ slug feet}^2,$$

$$I_y = 3{,}499{,}632 \text{ slug feet}^2,$$

$$I_z = 523{,}009 \text{ slug feet}^2$$

where x, y and z represent the yaw, pitch and roll axes, respectively.

There are two significant differences in these values as compared with the principal moments of inertia of the wet workshop. First, the gravity-gradient term α_z^2 in equation (2) is reduced to 18.6% of its previous value. Thus, instead of a 10 deg. oscillation, there would be approximately a 2 deg. roll axis oscillation. This smaller oscillation also serves to simplify the mathematical model for the system and to make the linearized model more accurate. Secondly, the principal moment of inertia about the roll axis, I_z, is more than twice as large as the previous value. This means that the change in velocity produced by a minimum impulse bit firing of the roll axis thrustors is less than half the value shown in Figure 8 and therefore that tighter control and increased accuracy are possible.

An investigation of the inertia tensor which applies to motions relative to the geometric axes indicates an increase in the yaw-roll coupling and in the angular difference between the geometric and principal axes. This could be offset by mixing the yaw and roll error signals as discussed in Section 3.

ACKNOWLEDGEMENT

The excellent assistance in programming and computation by Mrs. Nancy I. Kirkendall and Mrs. Barbara W. Lab is appreciatively acknowledged.

J. J. Fearnsides

1022-JJF-ulg

BIBLIOGRAPHY

1. Fearnsides, J. J., "Attitude Control for AAP 1/2 and AAP 2/3a: A Progress Report" - Case 620, B69 03026, Bellcomm, Inc. March 1969.

2. Chu, S. C., "Periodic Solutions of the Orbital Assembly Equations of Motion" - Case 620, B69 04021, Bellcomm, Inc. April 1969.

3. "Instrument Unit Applications for Saturn I Workshop," MSFC No. III-6-602-91, IBM No. 68-220-0002 (Volume II), July, 1968.

4. Kalman, R. E., Falb, P. L., and Arbib., M. A., "Topics in Mathematical System Theory," McGraw-Hill Book Company, New York, 1969.

5. Athans, M. and Falb, P. L., "Optimal Control," McGraw-Hill Book Company, 1966.

6. Sabroff, A. et al, "Investigation of the Acquisition Problem in Satellite Attitude Control," AD 628 062, TRW/Space Technology Laboratories, Redondo Beach, California, December, 1965.

7. Kalman, R. E., "The Theory of Optimal Control and the Calculus of Variations," in "Mathematical Optimization Techniques," R. Bellman (ed.), University of California Press, Berkely, Calif., 1963.

8. Arscott, F. M., "Periodic Differential Equations," The MacMillan Company, 1964.

9. Kalman, R. E. and Bertram, J. E., "Control Systems Analysis and Design via the Second Method of Lyapunov," Trans. ASME, J. of Basic Engr., Vol. 82, pp. 371-393, June, 1960.

10. Flügge-Lotz, I. and Craig, A., "The Choice of Time for Zeroing a Disturbance in a Minimum-Fuel Consumption Control Problem," Trans. ASME, J. of Basic Engr., pp. 29-38, March, 1965.

11. Busch, R. E. and Flügge-Lotz, I., "Attitude Control of a Satellite in an Elliptic Orbit, " AIAA Journal of Spacecraft and Rockets," Vol. 4, No. 4, pp. 436-442, April, 1967.

12. Pistiner, J. S., "On-Off Control System for Attitude Stabilization of a Space Vehicle," ARS Journal, pp. 283-289, April, 1959.

13. Elrod, B. D., "Evaluation of RCS Impulse Dispersions in Attitude Hold Modes," to be published as a Bellcomm Technical Memorandum.

14. Hough, W. W., Unpublished Notes, July, 1969.

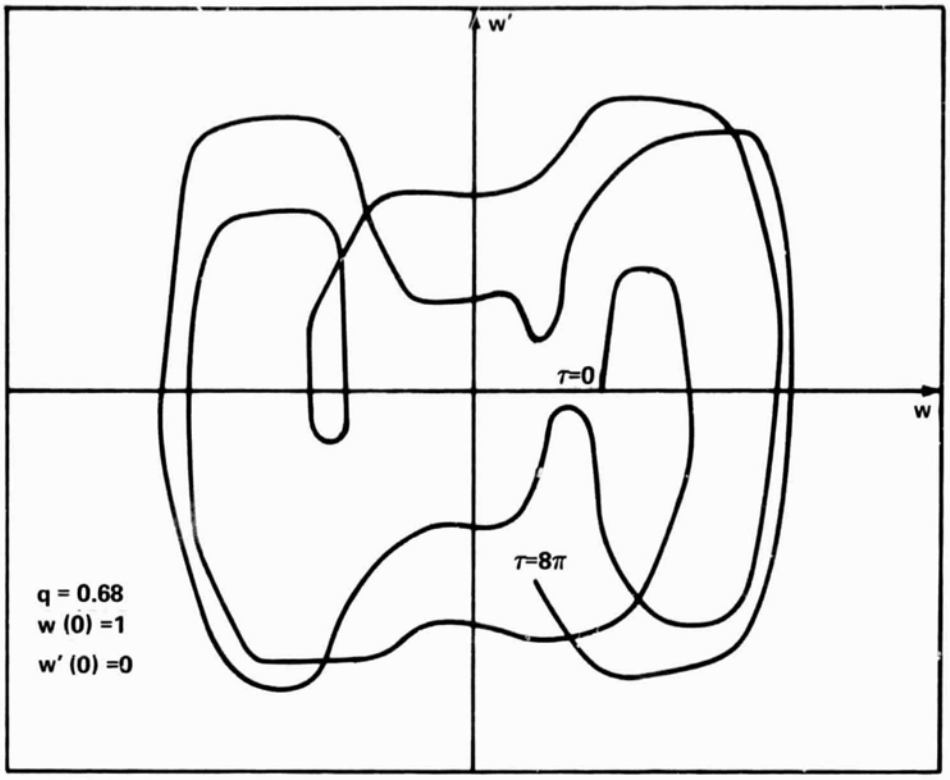

1a

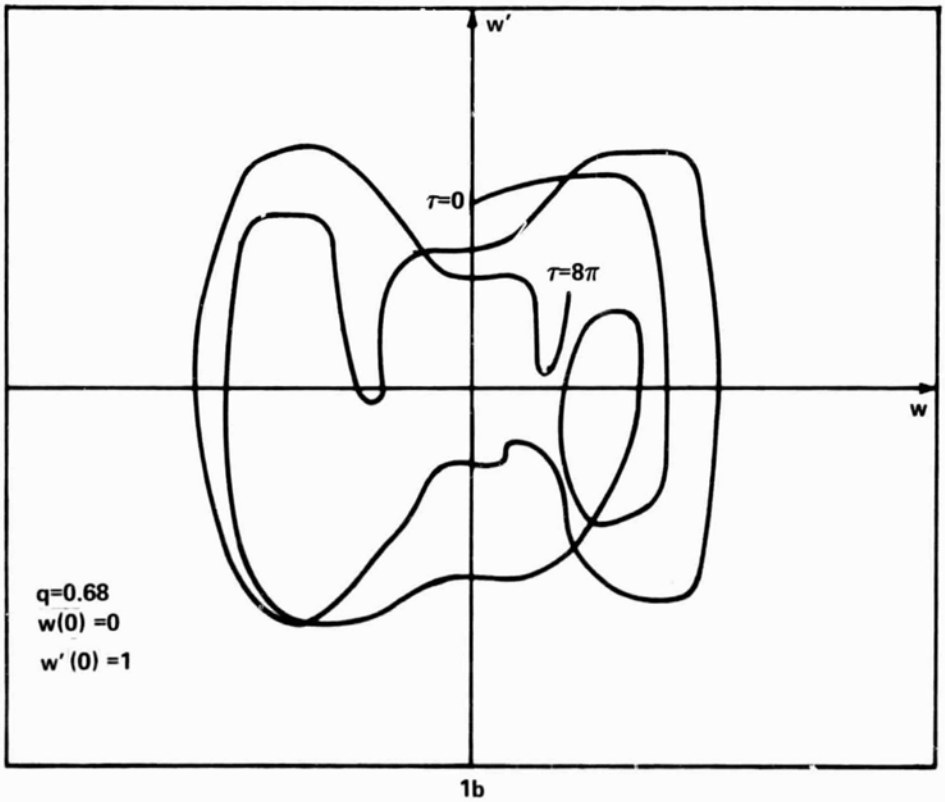

1b

FIGURE 1 - STATE SPACE TRAJECTORIES OF TWO SOLUTIONS TO THE MATHIEU EQUATION

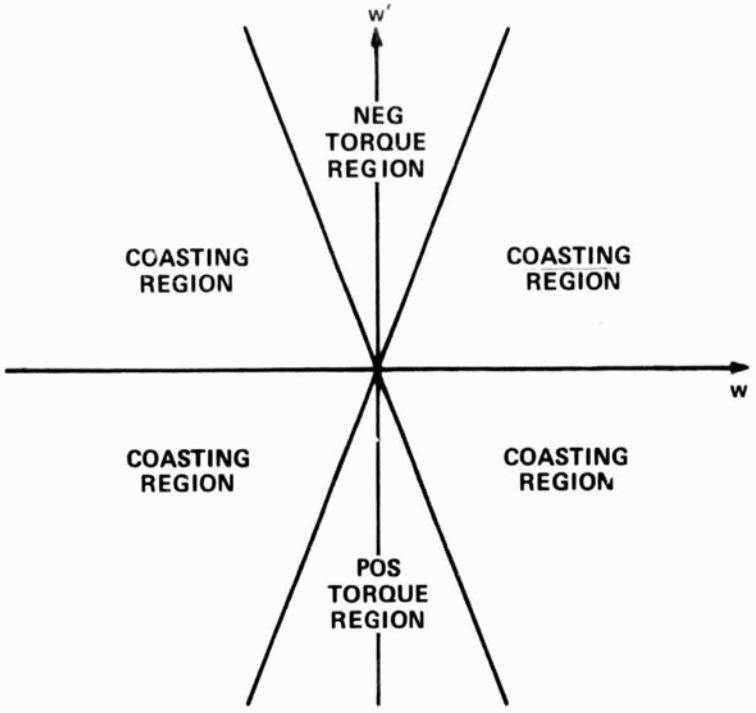

NOTE: TIME SCALE OF TORQUING REGIONS EXPANDED FOR CLARITY.

FIGURE 2 - OPTIMUM SWITCHING LINES IN W - W' PLANE

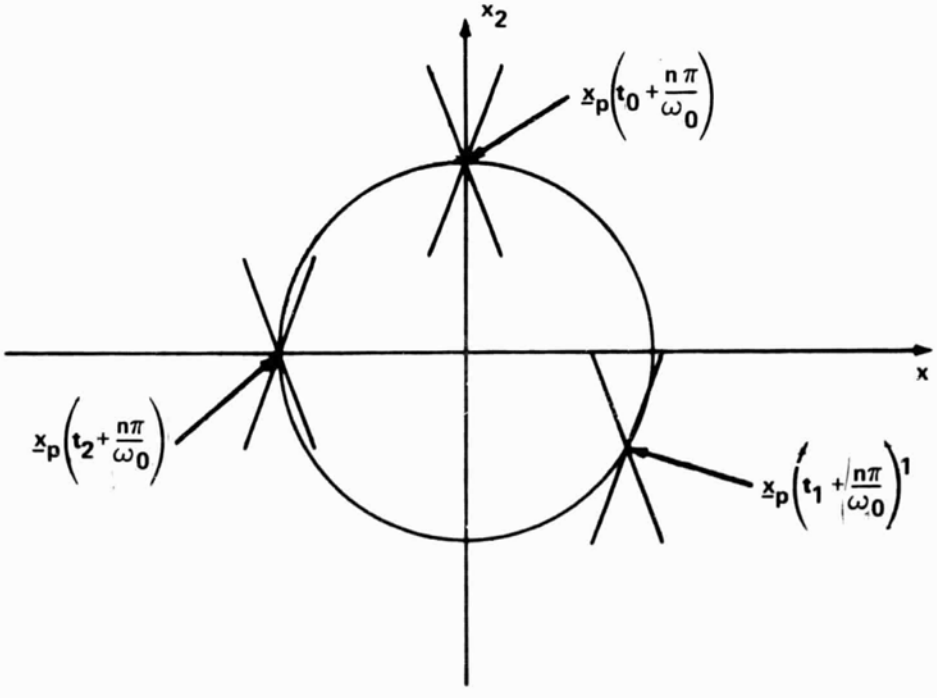

NOTE: 1. TORQUING & COASTING REGIONS AS IN FIGURE 2.
2. $t_0 < t_1 < t_2$; ω_0 = ORBITAL ANGULAR RATE

FIGURE 3 - OPTIMUM SWITCHING LINES IN X_1 - X_2 PLANE

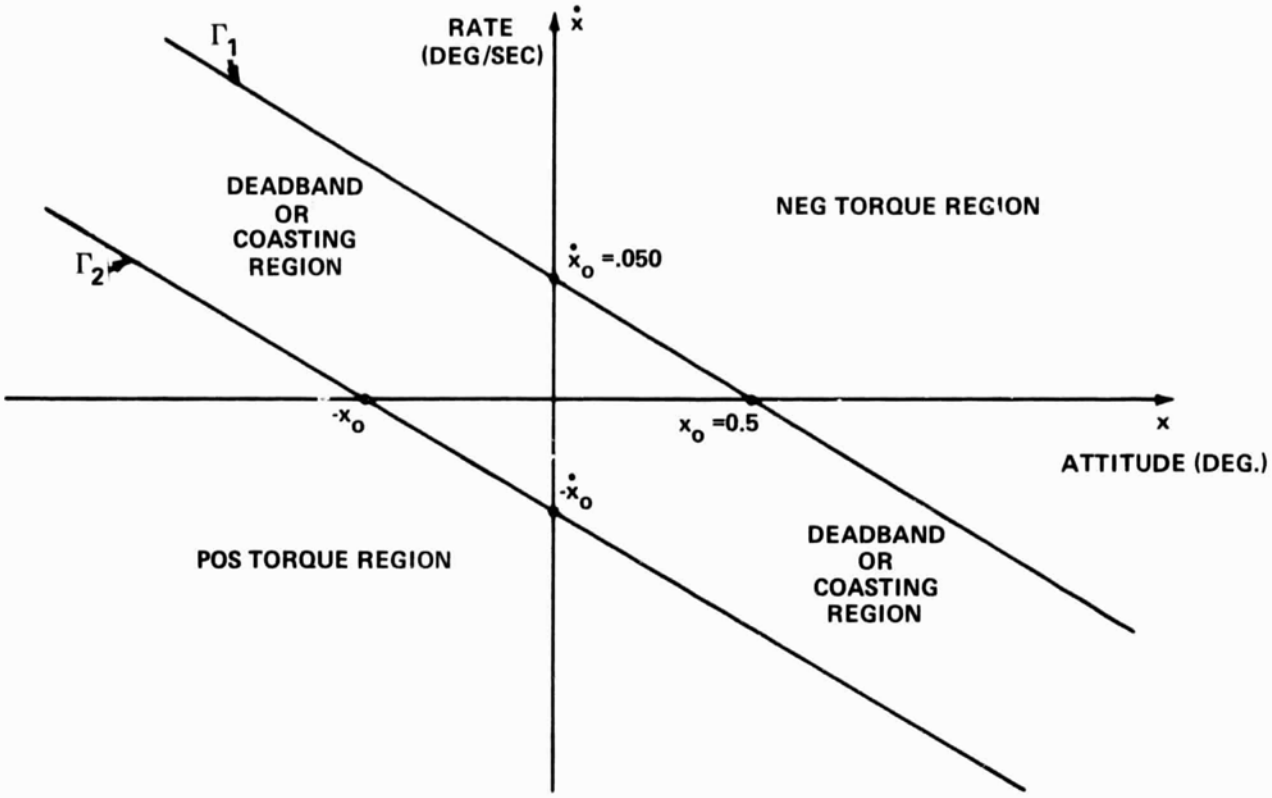

FIGURE 4 - SWITCHING LINES FOR NOMINAL CONTROL STRATEGY

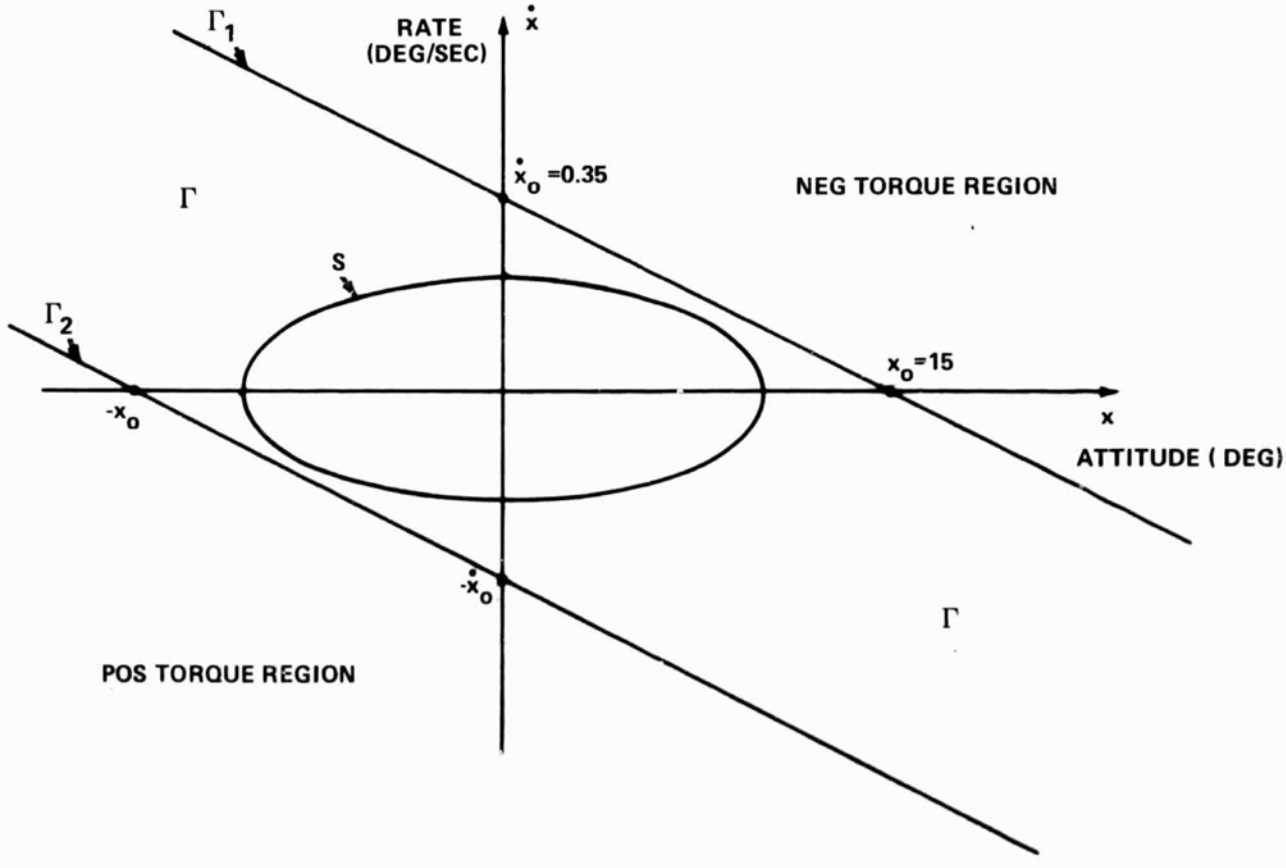

FIGURE 5 - SWITCHING LINES FOR THE EXPANDED DEADBAND METHOD

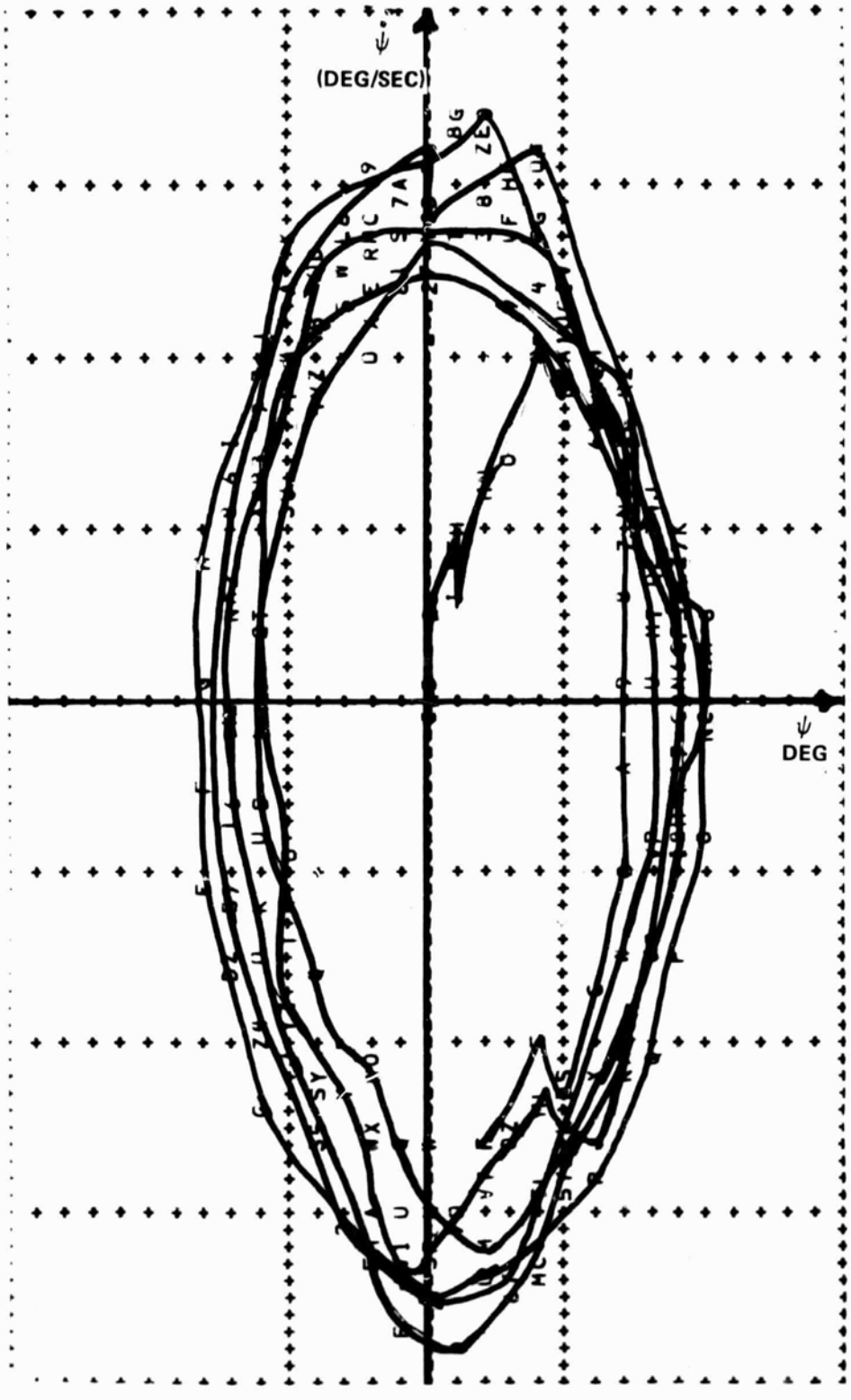

FIGURE 6 - A TYPICAL STATE TRAJECTORY OF THE EXPANDED DEADBAND METHOD

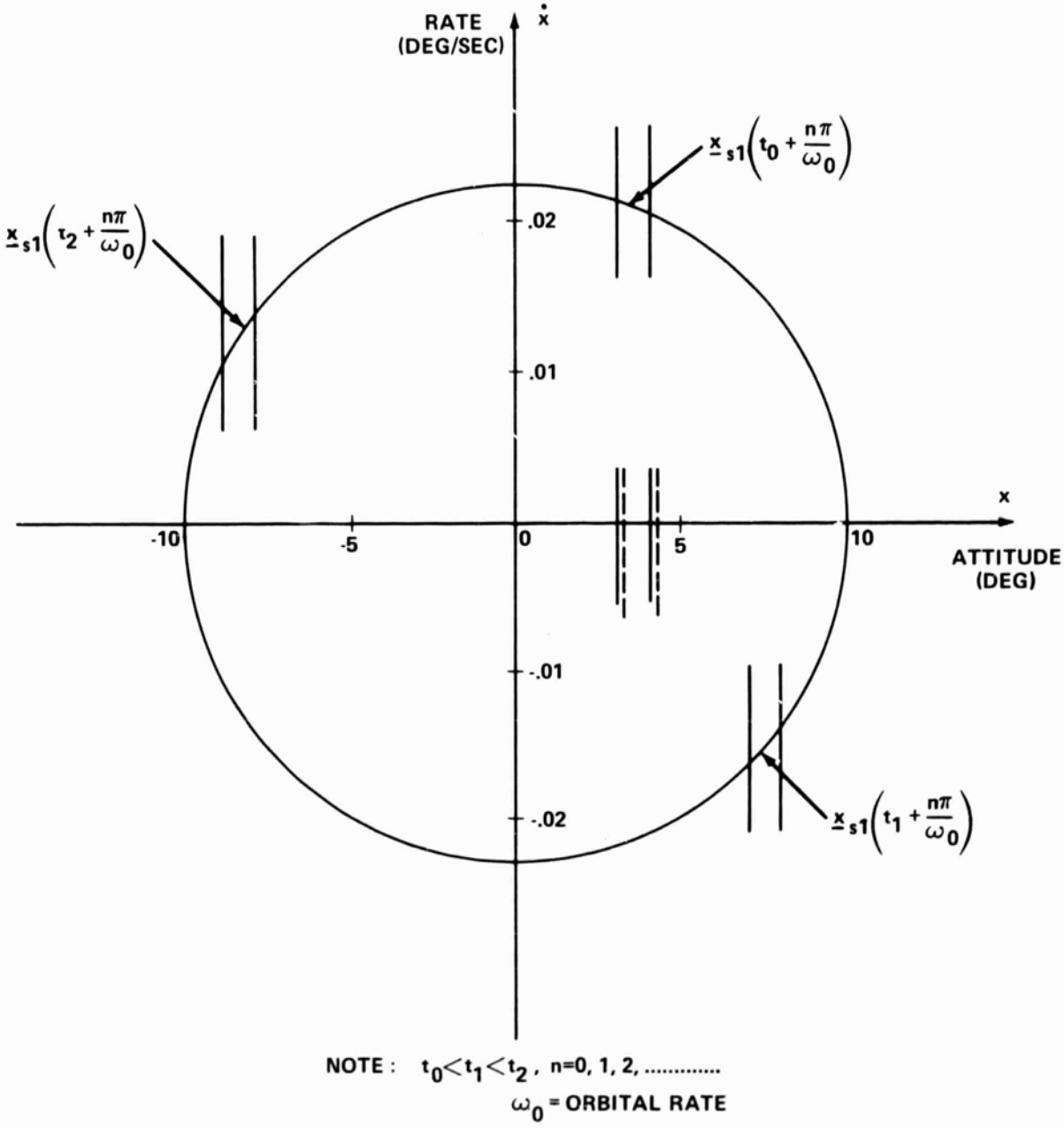

NOTE : $t_0 < t_1 < t_2$, n=0, 1, 2, ...

ω_0 = ORBITAL RATE

FIGURE 7 - SINUSOIDAL TRAJECTORY METHOD (STMI)
ATTITUDE AND RATE COMMAND

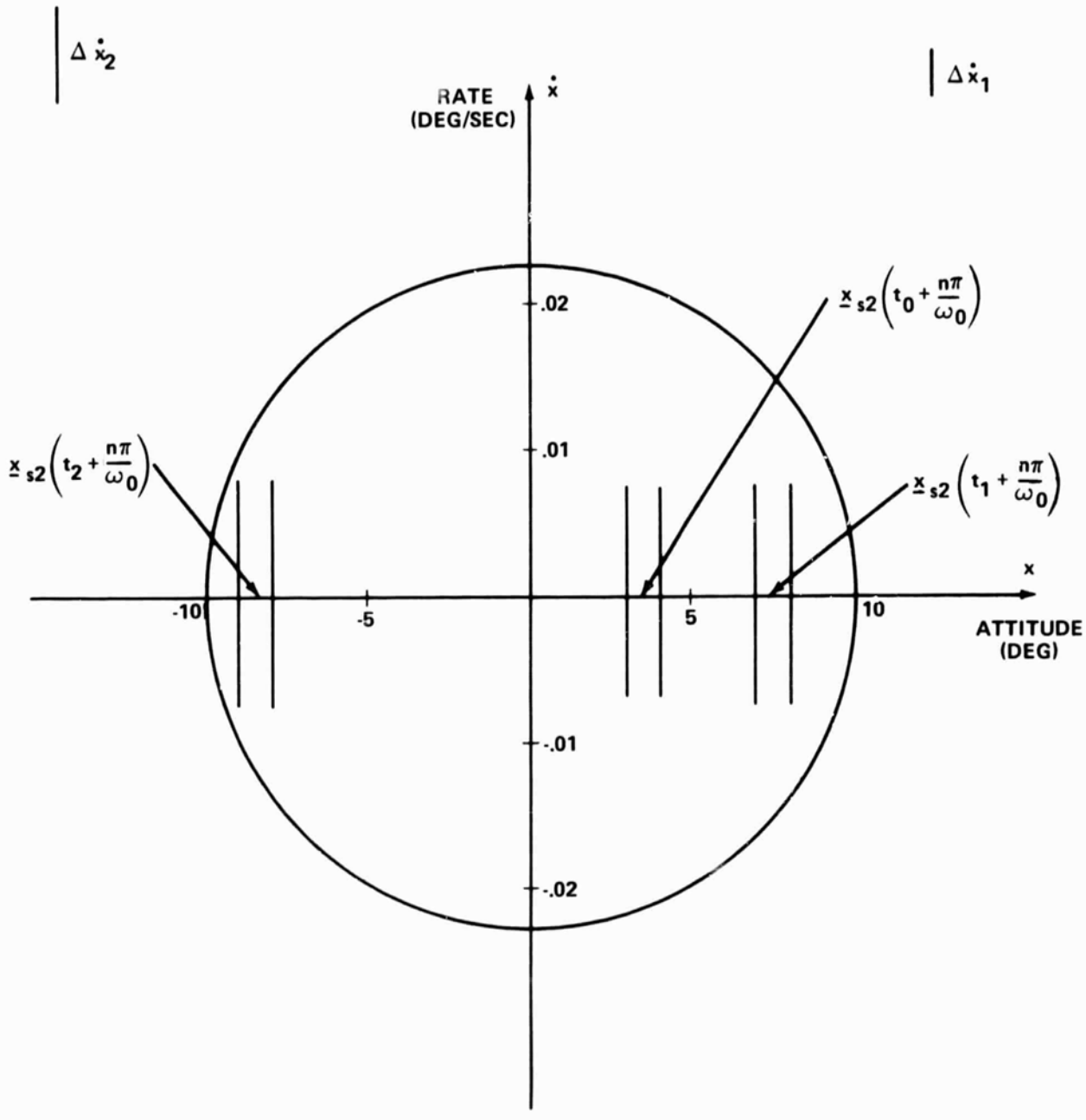

NOTE : $t_0 < t_1 < t_2$, n=0, 1, 2, ...

ω_o = ORBITAL RATE

FIGURE 8 - SINUSOIDAL TRAJECTORY METHOD (STMII)
ATTITUDE COMMAND

APPENDIX A

THE LINEARIZATION OF THE REGULATION PROBLEM

The equations of rotational motion of a spacecraft are, in general, nonlinear and can be written in the form

$$\dot{\underline{x}} = \underline{h}(\underline{x},t) + \underline{N}(\underline{x},t) \tag{A-1}$$

where $\underline{h}(\underline{x},t)$ and $\underline{N}(\underline{x},t)$ are mathematical models of the nonlinear plant dynamics and of the total gravity-gradient and aerodynamic torques acting on the plant, respectively. Expanding $\underline{h}$ and $\underline{N}$ in a Taylor series about $\underline{x}=\underline{0}$, which is an equilibrium point, yields

$$\underline{h}(\underline{x},t) = J_1(t)\underline{x} + \underline{\ell}(\underline{x},t)$$

and (A-2)

$$\underline{N}(\underline{x},t) = \underline{z}(t) + J_2(t)\underline{x} + \underline{m}(x,t) \quad ,$$

where:

$\underline{h}(\underline{0},t)=\underline{0}$ because $\underline{x}=\underline{0}$ is an equilibrium point,

J_1 and J_2 are matrices of first partial derivatives of $\underline{h}$ and $\underline{N}$ in $\underline{x}$, evaluated at $\underline{x}=\underline{0}$, and $\underline{\ell}(\underline{x},t)$ and $\underline{m}(\underline{x},t)$ have the property

$$\lim_{\underline{x}\to\underline{0}} \left\| \frac{\underline{\ell}(\underline{x},t)}{\|\underline{x}\|} \right\| = 0 \text{ and } \lim_{\underline{x}\to\underline{0}} \frac{\|\underline{m}(\underline{x},t)\|}{\|\underline{x}\|} = 0 \quad . \tag{A-3}$$

Using (A-6), the equation describing motions close to $\underline{x}_p$ can be written

$$\dot{\underline{\varepsilon}} = F(t)\underline{\varepsilon} + \underline{n}[(\underline{x}_p+\underline{\varepsilon}),t] \qquad \text{(A-9)}$$

The problem which remains is to determine when $\underline{n}(\underline{\phi},t)$ can be dropped from (A-9). When this can be done, (A-8) becomes linear and homogeneous. Consider expanding $\underline{n}[(\underline{x}_p+\underline{\varepsilon}),t]$ about $\underline{x}_p$. That is, write

$$\underline{n}[(\underline{x}_p+\underline{\varepsilon}),t] = \underline{n}(\underline{x}_p,t) + J_3(\underline{x}_p,t)\underline{\varepsilon} + \underline{o}(\underline{x}_p,\underline{\varepsilon},t) \quad , \qquad \text{(A-10)}$$

where J_3 is a matrix of first partial derivatives of $\underline{n}$ in $\underline{x}$ evaluated at $\underline{x}_p$, and $\underline{o}(\underline{x}_p,\underline{\varepsilon},t)$ has the property

$$\lim_{\underline{\varepsilon}\to\underline{0}} \frac{\|\underline{o}(\underline{x}_p,\underline{\varepsilon},t)\|}{\|\underline{\varepsilon}\|} = 0 \quad .$$

A properly linearized version of (A-9) is, then,

$$\dot{\underline{\varepsilon}} = F(t)\underline{\varepsilon} + J_3(\underline{x}_p,t)\underline{\varepsilon} + \underline{n}(\underline{x}_p,t) \quad . \qquad \text{(A-11)}$$

Note that the reason for the presence of $\underline{n}(\underline{x}_p,t)$ is that $\underline{x}_p(t)$ is the solution of the linearized equation (A-6) rather than (A-4). Also note that $\underline{\varepsilon}=\underline{0}$ is not an equilibrium point.

These concepts are now applied to the roll axis equation of the OWS. Recall that equation (3) is not an approximation of the full equations of motion which kept or discarded terms based on the criterion of linearity. Instead, terms which contributed more than 2% to the total angular acceleration corresponding to the solution of (2) were kept regardless of linearity. This leads to the assumption that the trajectory $\underline{x}_p(t)$ (A-6) is very close to the trajectory $\underline{\phi}(t)$ (A-7) and that $\underline{n}(\underline{x}_p,t)$ in (A-11) may be

neglected. The same argument can also be applied to assume that $J_3(\underline{x}_p, t)$ is small relative to $F(t)$.

The foregoing assumptions are made in order that an analytical model may be developed for the regulation problem. This model, in turn, is used as the criterion against which the design of two sub-optimal strategies is compared. One way of verifying the assumption that $\underline{x}_p(t)$ may be considered a solution of the nonlinear equation and $\underline{n}$ may be neglected is to develop the initial conditions for the periodic solution of (A-6), $\underline{x}_p(t)$, and use them in (A-7). The solution to the nonlinear initial value problem could then be compared with $\underline{x}_p(t)$. This has been done successfully for principal axis control (2) but a small variation in the definition of λ_B in (3) is necessary to obtain the same performance when the geometric axes are controlled. The 2% criterion used to establish (3) is too large for any constant terms that may arise. This is due to the long duration of time over which the equations of motion are integrated.

A practical verification of these assumptions could be made a posteriori by incorporating the control law which evolves from the analytical model into the OWS simulation and observing its performance. However, since the implementation of the optimal control strategy would require some nontrivial changes in the existing WACS design and since the easily-implemented suboptimal strategies work well relative to the original (nominal) WACS control law, this will not be done at this time. What follows then is based on these assumptions.

The dynamical system which will be used to represent the roll motion of the spacecraft near the desired trajectory is then

$$\dot{\underline{\varepsilon}} = F(t)\underline{\varepsilon} \quad ,$$

and with the control vector added is

$$\dot{\underline{\varepsilon}} = F(t)\underline{\varepsilon} + G(t)\underline{u} \qquad \text{(A-12)}$$

where, as before (4),

$$F(t) = \begin{bmatrix} 0 & 1 \\ 2\gamma_z^2 \cos 2(\omega_0 t - \delta) & 0 \end{bmatrix} ,$$

and

$$G(t) = \begin{bmatrix} 0 & 0 \\ 0 & N \end{bmatrix} .$$

For the purpose of distinguishing motion relative to $\underline{x}_p(t)$ rather than relative to the origin, the vector $\underline{\varepsilon}$ is defined to be

$$\underline{\varepsilon} = \begin{bmatrix} \varepsilon_1 \\ \varepsilon_2 \end{bmatrix} = \begin{bmatrix} w \\ \dot{w} \end{bmatrix}$$

The equivalent second order differential equation corresponding to (A-12) is then

$$\ddot{w} - (2\alpha_z^2 \cos 2\omega_0 t) w = Nu(t) \qquad \text{(A-13)}$$

which is a form of the Mathieu equation.

APPENDIX B

SOME PROPERTIES OF THE SOLUTIONS OF MATHIEU EQUATIONS

The purpose of this Appendix is to present the properties of the solutions of Mathieu equations which demonstrate the absolute stability of solutions to equation (13). The standard form of the Mathieu equation is

$$\frac{d^2w}{d\tau^2} = w'' = -(a-2q\cos 2\tau)w \qquad \text{(B-1)}$$

Its properties are well known [8] and are presented without proof.

Theorem 1. Mathieu's equation always possesses two solutions $w_1(\tau)$ and $w_2(\tau)$ such that:

i. $w_1(\tau)$ is even and $w_2(\tau)$ is odd,

ii. $w_1(0) = w_2'(0) = 1$, $w_1'(0) = w_2(0) = 0$,

iii. $w_1(\tau \pm \pi) = w_1(\pi)w_1(\tau) \pm w_1'(\pi)w_2(\tau)$

iv. $w_2(\tau \pm \pi) = \pm w_2(\pi)w_1(\tau) + w_2'(\pi)w_2(\tau)$

v. $w_1(\tau)w_2'(\tau) - w_2(\tau)w_1'(\tau) = 1$

vi. $w_1(\pi) = w_2'(\pi)$

Theorem 2 (Floquet's Theorem). Mathieu's equation always has at least one solution $y(\tau)$ such that $y(\tau+\pi) = \sigma y(\tau)$, where σ is a constant which depends on the parameters of (B-1) and which may be real or complex.

Corollary 2.1. $y(\tau+\pi) = \sigma y(\tau)$ if and only if σ is so chosen that $|A - \sigma I| = 0$, where A is the matrix

$$A = \begin{bmatrix} w_1(\pi) & w_1'(\pi) \\ w_2(\pi) & w_2'(\pi) \end{bmatrix}$$

and I is the identity matrix.

Corollary 2.2. Mathieu's equation always has at least one solution of the form $e^{\mu\tau}p(\tau)$ where μ is a constant and $p(\tau)$ has period π.

Proof. The proof is given to show the relationship between μ and σ. From corollary 2.1,

$$y(\tau+\pi) = \sigma y(\tau) \ .$$

Letting $\sigma = e^{\mu\pi}$ and $p(\tau) = e^{-\mu\tau}y(\tau)$ implies that

$$p(\tau+\pi) = e^{-\mu(\tau+\pi)}y(\tau+\pi)$$

$$p(\tau+\pi) = e^{-\mu\tau}e^{-\mu\pi}\sigma y(\tau)$$

$$p(\tau+\pi) = e^{-\mu\pi}\sigma \mathbf{p}(\tau)$$

$$p(\tau+\pi) = p(\tau) \ .$$

Note. Theorem 2 and corollaries 2.1 and 2.2 are true not only for Mathieu's equation but for any linear homogeneous differential equation with period π.

Definition. Define the equation $|A-\sigma I| = 0$ given in corollary 2.1 as the periodicity equation, its two solutions σ_1 and σ_2 as periodicity factors, and the corresponding values μ_1 and μ_2 as periodicity exponents.

Theorem 3. The product of the periodicity factors of Mathieu's equation is unity.

Corollary 3.1. If μ is a periodicity exponent of Mathieu's equation,

$$\cosh(\mu\pi) = w_1(\pi) = w_2'(\pi).$$

Corollary 3.2. If a and q of equation (3.1) are real and μ is any periodicity exponent then either $Re(\mu) = 0$ or $Im(\mu)$ is an integer.

Proof. Theorem 3 is proved by expanding the periodicity equation and using properties v. and vi. of Theorem 1

$$|A-\sigma I| = 0 = \sigma^2 - \left[w_1(\pi)+w_2'(\pi)\right]\sigma_2 + \left[w_1(\pi)w_2'(\pi) - w_2(\pi)w_1'(\pi)\right] \quad .$$

Application of v. and vi. of Theorem 1 leads to

$$\sigma^2 - 2w_1(\pi)\sigma + 1 = 0 \quad . \qquad \text{(B-2)}$$

Thus the product of the roots $\sigma_1\sigma_2$ of (B-2) is equal to 1.

Corollary 3.1 is proved by substituting $e^{\mu\pi}$ for σ in in (B-2) and using vi. of Theorem 1.

If a and q are real, corollary 3.1 means that $\cosh(\mu\pi)$ is real. If $\mu = \alpha + i\beta$, then

$$\sinh(\alpha\pi)\ \sin(\beta\pi) = 0 \quad ,$$

which proves corollary 3.2.

The stability of the solutions of (B-1) is analyzed directly from corollaries 3.2 and 2.2. Consider the case of corollary 3.2 when $Re(\mu) = 0$. Then by corollary 2.2, a solution of Mathieu's equation can be written in the form

$$y(\tau) = e^{i\beta\tau}p(\tau) \quad ,$$

or since $p(\tau)$ is periodic with period π

$$y(\tau) = e^{i\beta\tau} \sum_{n=-\infty}^{\infty} c_n e^{2ni\tau}$$

$$y(\tau) = \sum c_n e^{i(2n+\beta)\tau} \quad . \qquad \text{(B-3)}$$

If β is irrational, $y(\tau)$ is bounded but not periodic for all initial times. This satisfies the conditions for uniform stability given in [9].

The parameters of the OWS lead to $a=0$ and $q=0.68$ in (B-1). This leads to a value of $\mu=i\beta$ by

$$\cosh(\mu\pi) = \cosh(i\beta\pi) = \cos\beta\pi = w_1(\pi) \quad .$$

When (B-1) was integrated on a digital computer with these values of a and q and initial conditions corresponding to i. and ii. of Theorem 1, the solutions took the form shown in Figure 1. The value of $w_1(\pi)$ was -.13 which leads to $\beta \simeq 0.46$. The solution $w_1(\tau)$, then, is of the form

$$w_1(\tau) = \sum_{n=-\infty}^{\infty} c_n e^{i(2n+.46)\tau} \quad .$$

Note that the smallest "frequency" occurs when $n=0$ and corresponds to a "period" of $\simeq 4.35\pi$ seconds. The graphs in Figure 1 are taken over 8π seconds.

APPENDIX C

NECESSARY CONDITIONS FOR OPTIMAL CONTROL

The Minimum Principle of Pontryagin [5]

Given system,

$$\dot{\underline{\varepsilon}} = F(t)\underline{\varepsilon} + G(t)\underline{u} \quad , \tag{C-1}$$

let $\underline{u}^*(t)$ be an admissible control which transfers $(\underline{\varepsilon}_0, t_0)$ to $(\underline{0}, t_1)$. Let $\underline{\varepsilon}^*(t)$ be the trajectory of (C-1) corresponding to $\underline{u}^*(t)$ and which has the appropriate boundary conditions, $\underline{\varepsilon}^*(t_0) = \underline{\varepsilon}_0$, $\underline{\varepsilon}^*(t_1) = \underline{0}$. In order that $\underline{u}^*$ be optimal for the cost functional,

$$J(\underline{u}) = \int_{t_0}^{t_1} \lambda |\underline{u}| dt \quad , \tag{C-2}$$

it is necessary that there exist a function $\underline{p}^*(t)$ such that:

$$\text{a.} \quad \dot{\underline{\varepsilon}}^* = \frac{\partial H}{\partial \underline{p}} [\underline{\varepsilon}^*, \underline{p}^*, \underline{u}^*, t] = F(t)\underline{\varepsilon}^* + G(t)\underline{u}^*$$

$$\dot{\underline{p}}^* = -\frac{\partial H}{\partial \underline{\varepsilon}} [\underline{\varepsilon}^*, \underline{p}^*, \underline{u}^*, t] = F^T(t)\underline{p}^* \tag{C-3}$$

with the boundary conditions specified above and where H (the Hamiltonian of the system) is defined by

$$H(\underline{\varepsilon},\underline{p},\underline{u},t) = \lambda|u| + \underline{p}\cdot(F(t)\underline{\varepsilon}+G(t)u). \qquad (C-4)$$

b. $H[\underline{x}^*,\underline{p}^*,\underline{u}^*,t] \leq H[\underline{x}^*,\underline{p}^*,\underline{u},t]$

c. The function $H(\underline{x}^*,\underline{p}^*,\underline{u}^*,t)$ satisfies relations

$$H[\underline{x}^*,\underline{p}^*,\underline{u}^*,t] = -\int_t^{t_1} \frac{\partial H}{\partial t}\,[\underline{x}^*(\tau),\underline{p}^*(\tau),\underline{u}(\tau),\tau]d\tau$$

and

$$H[\underline{x}^*(t_1),\underline{p}^*(t_1),\underline{u}^*(t_1),t_1] = 0$$

where t_1 is the unspecified terminal time.

For system (12):

$$H(\underline{\varepsilon},\underline{p},\underline{u},t) = \lambda[|u|+p_2u] + p_1x_2 + (2q\cos 2\tau)p_2x_1 \quad . \qquad (C-5)$$

Condition b. implies the control law,

$$u^* = \begin{cases} 0 \ , & |p_2^*| < 1 \\ -1 \ , & p_2^* > 1 \\ 1 \ , & p_2^* < -1 \end{cases} \quad \triangleq -cst\{p_2^*\} \qquad \text{(C-6)}$$

where cst is called the "coasting" function. Condition a. provides the interesting result that p_2^* satisfies equation (12). Condition c. and the properties of solutions of (12) can be used to demonstrate that

$$p_2^*(t_1) = \begin{cases} -1 \ , & u = 1 \\ \\ 1 \ , & u = -1 \ . \end{cases} \qquad \text{(C-7)}$$